8.5 CONVECTIVE WINDS AT THE FLORIDA SPACEPORT: YEAR-3 OF PLYMOUTH STATE RESEARCH

Heather A. Dinon, Matthew J. Morin and James P. Koermer*
Plymouth State University, Plymouth, New Hampshire

William P. Roeder
45th Weather Squadron, Patrick Air Force Base, Florida

1. Introduction

The USAF 45th Weather Squadron (45 WS) provides comprehensive weather support to America's space program at Cape Canaveral Air Force Station (CCAFS) and NASA Kennedy Space Center (KSC) (Harms et al. 1999). These facilities are in east central Florida, within 'Lightning Alley' of the U.S. As a result, thunderstorms and their associated hazards especially lightning and convective winds, are one of the largest operational concerns of the 45 WS. Convective wind warnings are the second most frequent type of weather advisory issued by the 45 WS forecasters for this area (Wheeler and Roeder 1996). The thresholds for the 45 WS convective wind warnings are $\geq$ 35 kt, $\geq$ 50 kt, and $\geq$ 60 kt, from surface to 300 ft, with lead-times of 30 min to 60 min. The Plymouth State University (PSU) research team has focused on providing an improved warm-season convective wind climatology and other tools that can be used by 45 WS forecasters.

Loconto et al. (2006) presented the results of the initial climatological study based on five-minute averaged peak wind speed for over 40 wind tower sites sampling up to 10 height levels from the CCAFS/KSC mesonetwork (Case and Bauman 2004). Other data used included highly detailed surface observations from KTTS (the Shuttle Landing Facility) and other nearby surface METAR observations; KXMR radiosonde soundings; the WSR-88D radar at Melbourne, FL; and satellite imagery. Besides the convective wind climatology, this paper also reported on some preliminary work investigating thermodynamic indicators and profile differences. Loconto (2006) went into much greater depth in evaluating various operationally used forecast techniques, T1, T2, WINDEX, and MDPI indices; examined differences in thermo-dynamic profiles; and evaluated a currently used radar gust equation and proposed improvements that should significantly reduce false alarm rates.

During the second year of this convective wind study, two additional warm seasons of data (2004 and 2005) were added to the climatology. This research also focused on expanding the convective periods to encompass all episodes rather than just those exceeding the warning criteria. The resulting climatology was stratified by year, month, time-of-day, tower elevation, tower, wind direction, wind speed, and prevailing synoptic flow regimes. Additionally, the frequency distributions of peak wind speeds were expanded and best-fit Gumble curves were determined and integrated to provide the probability of the 45 WS convective wind warning criteria being satisfied ($\geq$ 35 kt, $\geq$ 50 kt, and $\geq$ 60 kt).

The PSU team also did a very preliminary study with the GPS Integrated Precipitable Water (IPW) data from the Cape Canaveral Coast Guard Station and found that though it may be useful as a forecast tool, more data and study were needed. Cloud-to-Ground Lightning Surveillance System (CGLSS) flash density data (Boyd et al. 2005) were also examined for most of the convective periods and there was a direct correlation between peak convective wind strengths and the number of lightning strikes. Some preliminary exploration was done on the issue of time lag between the first 20 knot peak wind report and the first 35 knot or greater report. It was found that a lag of at least 30 minutes was present nearly 60% of the time. All of these second year PSU results are summarized in more detail by Cummings et al. (2007).

A significant addition to the climatology during the summer of 2007 was the inclusion of WSR-88D radar Level-III data, primarily base reflectivity and vertically integrated liquid (VIL), for Melbourne (MLB) and Tampa (TBW). These data were not readily accessible during previous years and the available radar data used back then were quite poor in their time and space resolution. This paper demonstrates how these new radar data have improved the climatology and how they have

*Corresponding author address: *Dr James P. Koermer, MSC #48, Dept. of Chemical, Earth, Atmospheric and Physical Sciences, Plymouth State University, Plymouth, NH, 03264; e-mail: koermer@plymouth.edu*

helped to identify trends in the setup and behavior of convective activity in the wind tower mesonetwork on the Florida Space Coast.

2. Convective Period Identification

For the purposes of this research, we use the convective period definition that was previously defined by Cummings et al. (2007) as "a period of convective activity with at least a 6-hour break of no convection before and after the period. Start time was noted as the top of the hour when convection first occurred and end time was noted as the top of the hour after the last evidence of convection."

Convective periods identified for this region and time frame from previous studies were further refined based on additional review of the NEXRAD MLB data (with backup for missing data provided from the TBW site). A few periods were dropped and a few were added. Start/end times were also fine tuned. As before, synoptically driven pressure gradient cases, including those from nearby tropical cyclones were also eliminated from this study.

The net results for the months of May through September of the 11-year (1995-2005) study are listed in Table 1, which shows that 35% of the convective periods have warning level peak winds (≥ 35 kt), but only 7% of all convective events have winds exceeding 50 knots and only 1.2% exceed 60 knots.

Table 1. Warm season convective period identification results for May-September from 1995 through 2005.

QUANTITY	NUMBER	%
Total convective periods	773	100
Periods with winds ≥ 35 knots	273	35
Periods with winds ≥ 50 knots	52	7
Periods with winds ≥ 60 knots	9	1.2

The average annual number of convective periods is approximately 70 per year. The convective periods cover roughly 7000 hours, which is well over 600 hours per year, equating to about 18% of the possible hours. Although the majority of these events occur during the afternoon and early evening hours, a strong wind event can occur at almost any time of day (Cummings et al. 2007).

3. Blending of Radar and Wind Tower Data

The radar data were closely time-matched to the highest 5-minute peak wind observation at or below 300 feet for each individual tower in the CCAFS/KSC mesonetwork (See Figure 1) for all of the 773 identified convective periods. Over 84,000 custom wind files were created that matched closely with the radar observation times. A web-based application was developed by the team to generate still and/or loop overlays of these wind data geo-located over the corresponding radar imagery. Images showing the radar/wind overly capabilities will be shown with various case studies presented later in this paper.

The radar images overlaid with the high time and spatial resolution wind data show the development and propagation of convective winds throughout the study area for a particular event. The radar data and overlaid wind speeds were essential for determining which exact cell or group of cells caused the high winds. Results also indicate the importance of collision events, such as cell mergers and outflow boundary/sea breeze front interactions, in triggering most of the strong (≥ 50 knots) convective wind events.

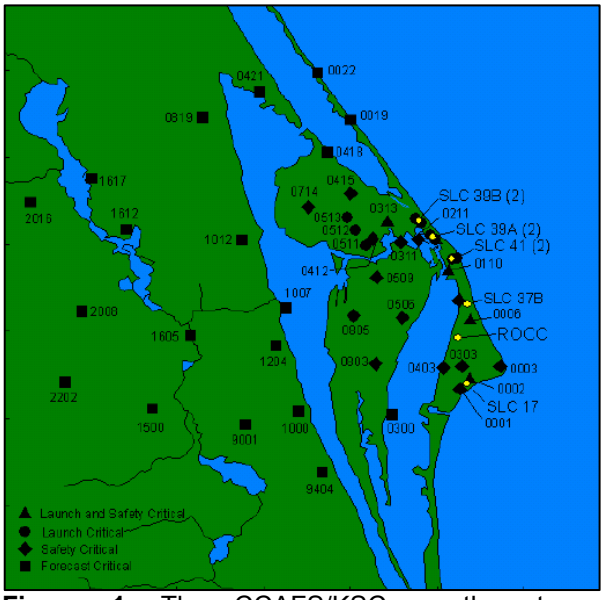

Figure 1. The CCAFS/KSC weather tower mesonetwork.

4. Radar/Wind Study Methodology

To produce a thorough radar/wind summary for warning criteria events, we considered the variables of cell initiation, cell structure, cell strength, direction of movement, and location of maximum peak wind.

Cell initiation describes the mesoscale setup that causes the cell to develop to the intensity where it produces a warning level criteria maximum peak wind. Cell initiation factors consist

of cell development due to a sea breeze front, outflow boundary, or the combination of the two boundaries. It is not necessary for there to be a sea breeze front or an outflow boundary for there to be strong thunderstorms. Therefore, a fourth category was created that would encompass all events where no sea breeze front or outflow boundary was present.

Cell structure describes the organization of the cell or cells at or near the time of the maximum peak wind. The categories used were line, cluster, and individual cell.

Cell strength takes into account the size of the area with the highest reflectivity and its continuity. The categories were weak/broken (< 45 dBZ), moderate (45-55 dBZ), and strong (> 55 dBZ).

It is frequently observed that the direction of a system of cells has a different trajectory than the embedded cells within the system. Therefore, cell group and individual cell movements were both considered. Each type of movement was stratified into one of 16 cardinal wind directions.

The last variable used in this study describes the location of the reported maximum peak wind with respect to the cell believed to have caused the high wind speed. The categories were behind, overhead, and ahead of the tower that reported the maximum peak wind.

5. Results

5.1. Radar Summary for Warning Criteria Events

A thorough analysis of radar and overlaid wind tower data was used to create a radar summary for all events where the maximum peak wind speed equaled or exceeded warning level criteria (≥ 35 knots). While we are still working to analyze all events, a subset of 139 events, meeting this criterion, was identified. Three events had to be excluded due to missing radar data from both MLB and TBW radar sites. The sample size of 136 events, nearly half of the warning level events, was deemed acceptable to develop preliminary statistics on the cell initiation, structure, strength, trajectories, and location.

Investigation of several years of warm season convective periods led to the classification of four main types of cell initiation scenarios: sea breeze front and outflow boundary interaction (SBF & OFB), outflow boundary only (OFB only), sea breeze front only (SBF only), and no boundary interaction (No SBF or OFB). Figure 2 shows that the most frequent category (52 out of 136 events or 38%) was a sea breeze front and outflow boundary interaction which caused cells to develop and intensify. On the other hand, no boundary interaction was needed to produce a warning criteria wind speed 27% of the time. Outflow boundary cell initiation and sea breeze front cell initiation occurred 18% and 16% of the time, respectively. The strong dependence on boundary interaction is not surprising since "secondary convection" (convection forming from previous convection) has long been known to be conducive to downburst formation (Mackey 1998; Wheeler and Roeder 1996).

Cell structure was one of the most statistically significant parameters of this study. Figure 3 demonstrates the high frequency that a line of cells causes strong convective winds. Some type of linear structure, be it quasi-linear or even bowed, occurs 71% of the time. A cluster of cells accounts for 23% of the events while an individual cell only occurs 6% of the time when there is a high maximum peak wind.

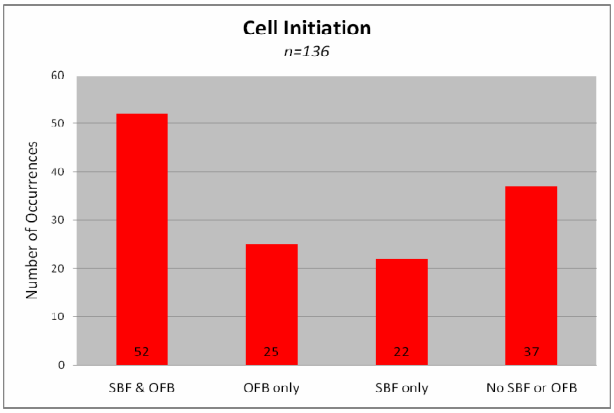

Figure 2. Frequency of the different scenarios of cell initiation corresponding to warning-level events where SBF = sea breeze front and OFB = outflow boundary.

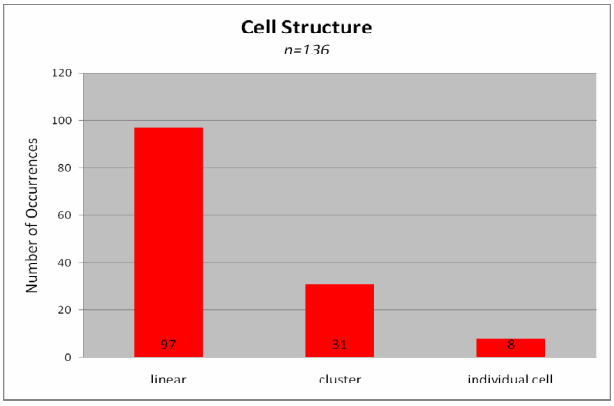

Figure 3. Frequency of the three types of cell formations corresponding to warning-level events.

Figure 4 shows that moderate (45-55 dBZ) and strong (> 55 dBZ) convective cells in Florida are associated with 75% of the high wind speed events. However, it was seen that weak cells also had the ability to produce warning-level criteria wind speed events

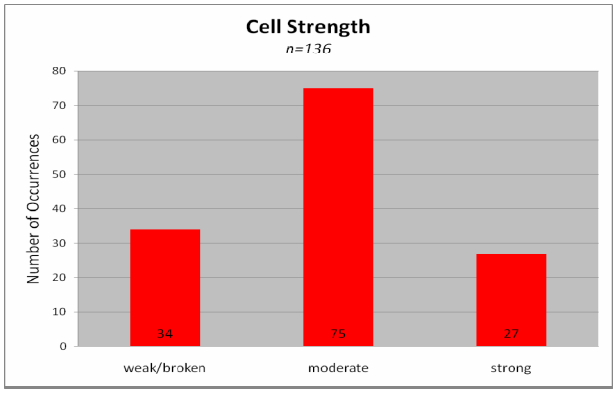

Figure 4. Frequency of the three types of cell strength (weak/broken < 45 dBZ, moderate = 45-55 dBZ, and strong > 55 dBZ).

Figures 5 and 6 show the number of events versus movement, considering cell groups and individual cells separately. In both cases, cells traveling eastward produce the largest number of high maximum peak wind speeds. This may be an artifact that eastward moving cells tend to be stronger, since they usually have been gathering strength from the Sun heated land while moving across the Florida peninsula throughout the day. The only noticeable difference between group and individual cell movement is that the groups of cells tend to head east while the embedded individual cells tend to head towards the east-northeast.

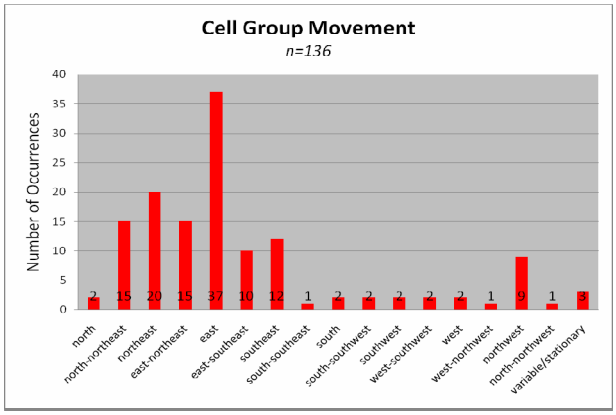

Figure 5. Frequency of the direction of cell group movement. Directions represent the direction toward which the group is heading, e.g. an 'east' moving group is moving from west to east.

These figures also show how rare it is for cells moving westward to produce high winds, which was previously noted by Cummings et al. (2007). The direction of movement was between north and south-southeast 82% of the time while only occurring 17% of the time between the directions of south and north-northwest (1% of the directions were either variable or the cells were stationary).

In 83% of the events, the cell that caused the maximum peak wind was over the tower that reported the wind speed (Figure 7). Otherwise the tower was either ahead of or behind the cell 12% and 5% of the time, respectively. This strongly suggests that convective winds lose their intensity rapidly with distance, at least compared with the tower spacing in the CCAFS/KSC mesonetwork.

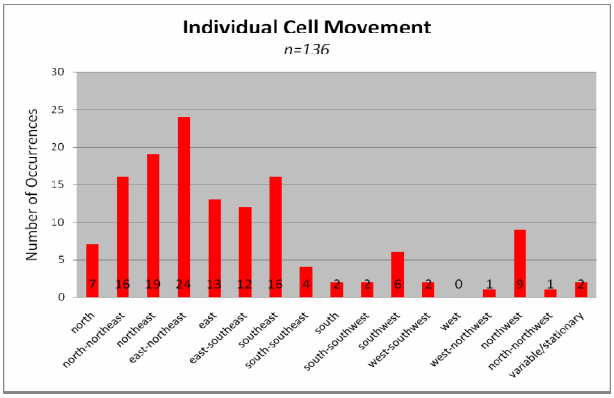

Figure 6. Frequency of the direction of individual cell movement. Directions represent the direction toward which the cell is heading, e.g. a 'west' cell is moving from east to west.

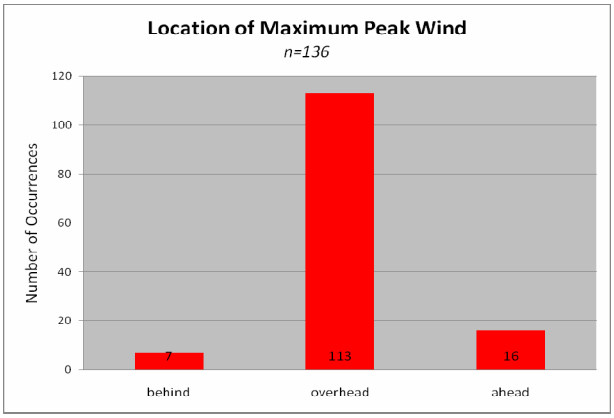

Figure 7. Frequency of the location maximum peak winds with respect to the cell.

Most of the time, the magnitude of the maximum peak wind speed made sense given cell structure and strength. However, there were a few occasions when there was either a high peak wind speed with a weak convective cell setup or a low

peak wind speed with a strong convective cell setup. For these events, Cape Canaveral, Florida (KXMR) radiosonde data from Global Systems Division and University of Wyoming's radiosonde sites were analyzed. For the instances where the maximum peak wind was much stronger than expected, the sounding indicated an unsaturated layer from the surface to around 925 hPa with a saturated layer above. In this type of scenario, downdrafts were accelerated by increased negative buoyancy due to evaporative cooling.

For the instances where the maximum peak wind was much weaker than expected, there was a thinner than normal unsaturated layer at the surface and a thicker saturated layer above. The decreased opportunity for evaporative cooling seems to explain the instances where the maximum peak wind was much weaker than expected, perhaps combined with less negative buoyancy acting on the descending parcel in the boundary layer due to the boundary layer air being slightly denser from its lower humidity/lower virtual temperature. This feature was observed by Atkins and Wakimoto (1991) and modeled by Srivastava (1985) and Proctor (1989). Figure 8 shows this concept in graphical form.

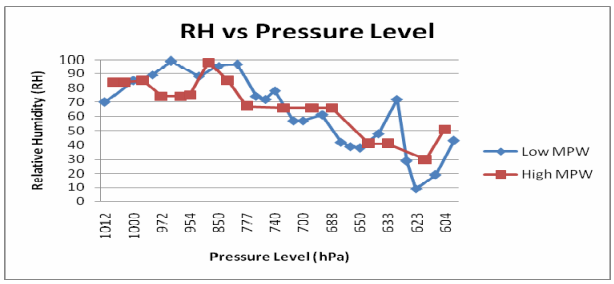

Figure 8. Differences in relative humidity at low to mid levels for a weak and strong maximum peak wind (MPW) event. Note the thicker unsaturated layer at low levels for the high peak wind event.

5.2. Case Studies

The three case studies that follow provide general examples of the conditions for well-above-criteria, at-criteria, and below-criteria peak wind events. Strong events frequently needed a sea breeze front and outflow boundary interaction to form moderate to strong lines of cells. Also noted in this case study, was the fact that all but one of the 30 high convective wind events had an eastward component to the cell movement, which reiterates the climatology performed in previous studies of KSC/CCAFS convective wind events by Cummings et al. (2007).

5.2.1. Well Above-criteria Maximum Peak Wind Event (greater than 50 knots)

The first case study investigated a convective wind event which took place on 3 May 1997. At 2025 UTC, the wind warning criteria of greater than or equal to 35 knots was greatly exceeded, with a maximum peak wind speed of 64 knots reported by Tower 421 in the mesonetwork. The event began with an area of airmass thunderstorms moving northeast from Central Florida. These cells eventually organized into a small cluster and then into a bowed line just before reaching the mesonetwork. Minutes before passing over Tower 421, the bowed line was rapidly intensified by an interaction with a sea breeze front heading west. The clash of the line of cells and the sea breeze front occurred just before Tower 421 reported the maximum peak wind. The radar image around the time of this interaction is shown in Figure 9. The WSR-88D/MLB radar indicated a maximum reflectivity of around 60 dBZ in the line of cells right after the peak wind was reported.

This case study is a good example of the conditions needed for a maximum peak wind speed greater than 50 knots. Eighty-seven percent of all analyzed events with greater than 50 knot winds had a sea breeze front and/or outflow boundary interaction. The cell structure was usually linear and had a strength of either "moderate" or "strong". All but one of the 30 high convective wind events had an eastward component to the cell movement. This corresponds to the climatology developed in the previous PSU studies of KSC/CCAFS convective wind events (Cummings et al. 2007).

5.2.2. At-criteria Maximum Peak Wind Event (around 35 knots)

The second case study investigated a convective wind event which took place on 28 August 2003. At 1800 UTC, the wind warning criteria was barely exceeded, with a maximum peak wind speed of 36 knots reported by Tower 3131.

The event began with a long line of cells heading northwest from the southeast coast of Florida. The line stretched across the entire radar viewing area (30 NM) and was mostly composed of weak individual convective cells. An outflow boundary was produced from a small group of more intense cells about two hours before the onset of the maximum peak wind. The outflow boundary spawned new cells which appeared to produce the 36 knot peak wind speed.

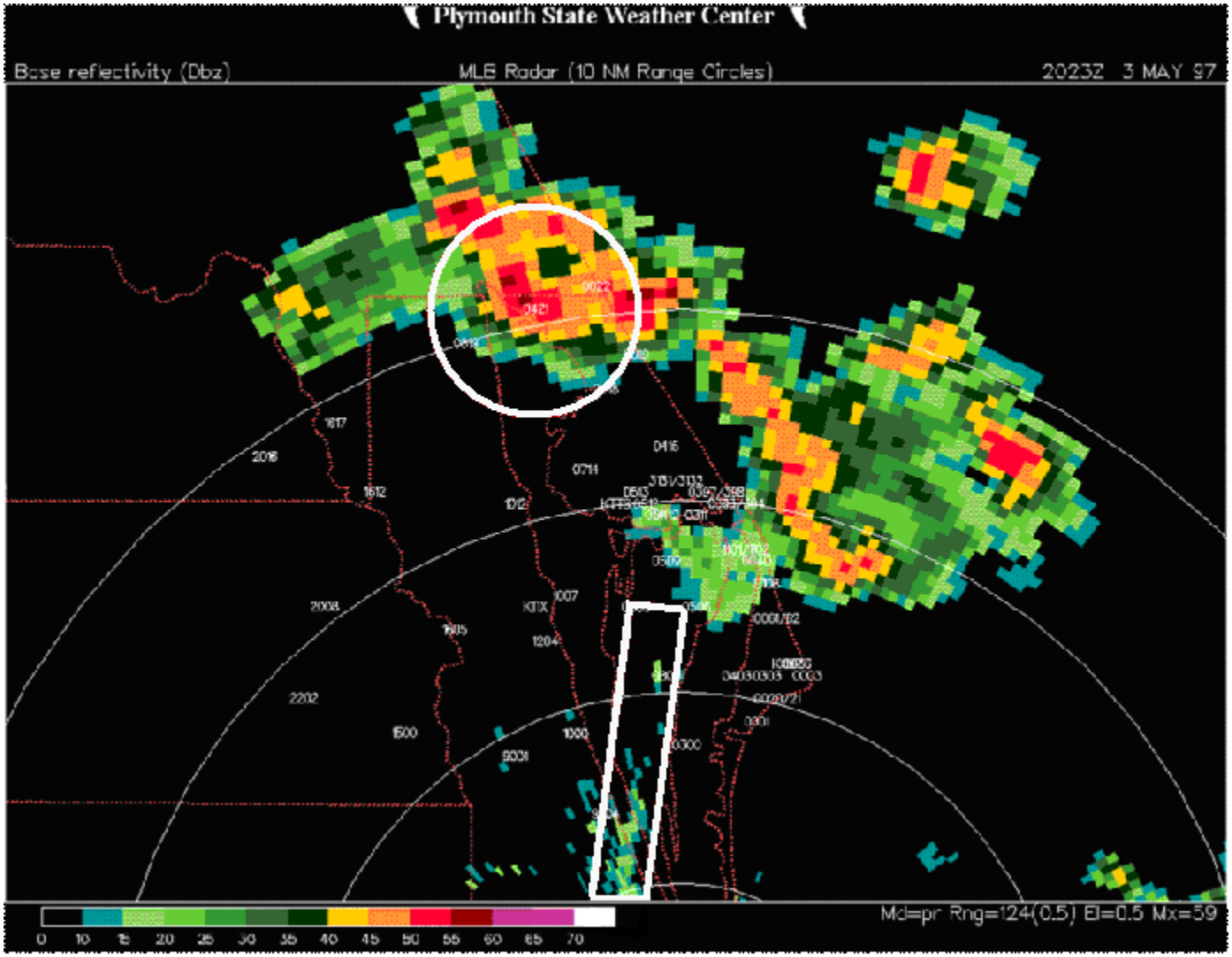

Figure 9. WSR-88D/MLB radar image around the time of the reported 64 knot maximum peak wind. White numbers plotted indicate tower ID. The white circle indicates the location of Tower 421, where the high wind speed was reported. The white rectangle shows evidence of the sea breeze front which was responsible for intensifying the bowed line of storms.

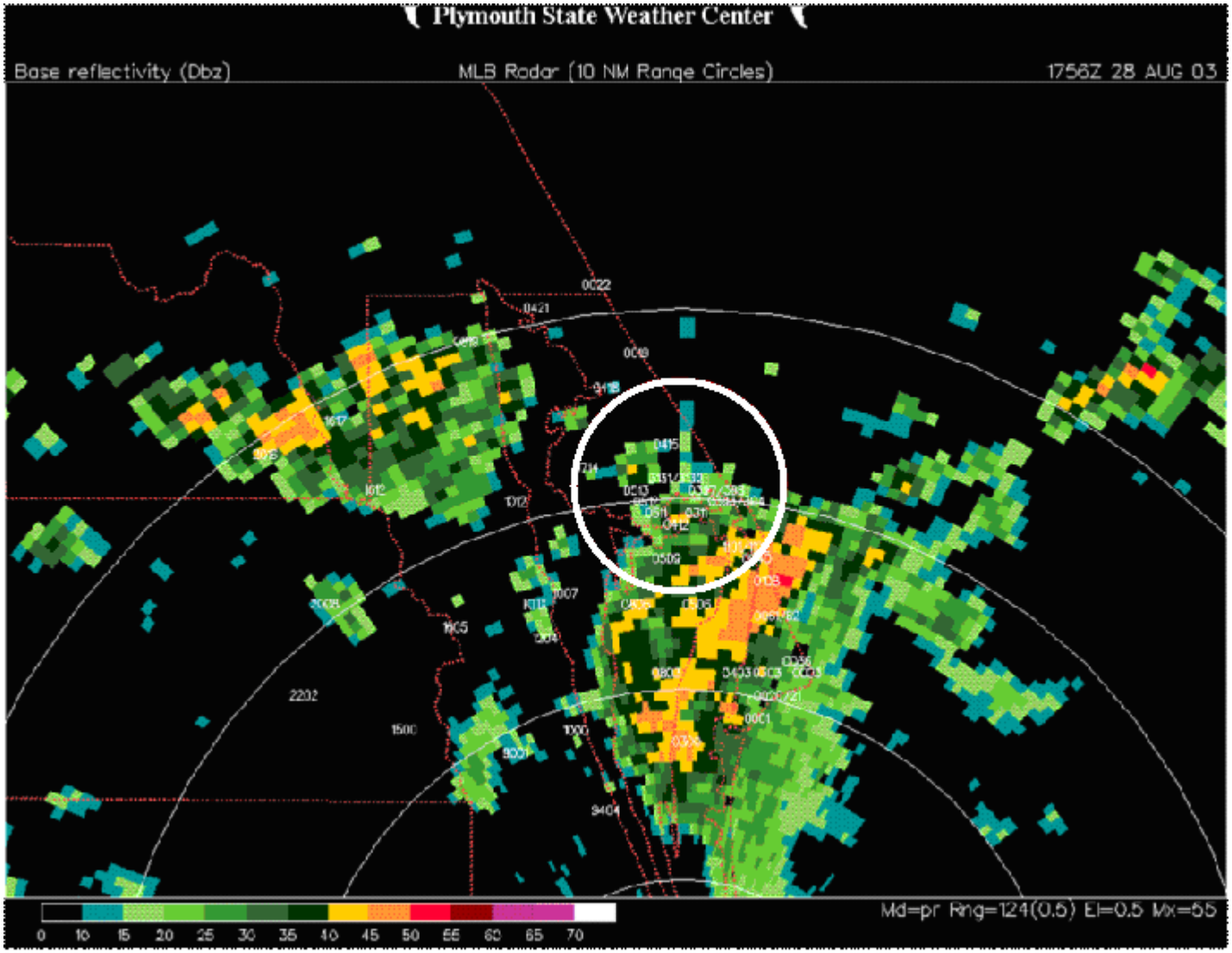

Figure 10. WSR-88D/MLB radar image around the time of the 36 knot maximum peak wind. White numbers plotted indicate tower ID. The white circle indicates the location of Tower 3131, where the high wind speed was reported.

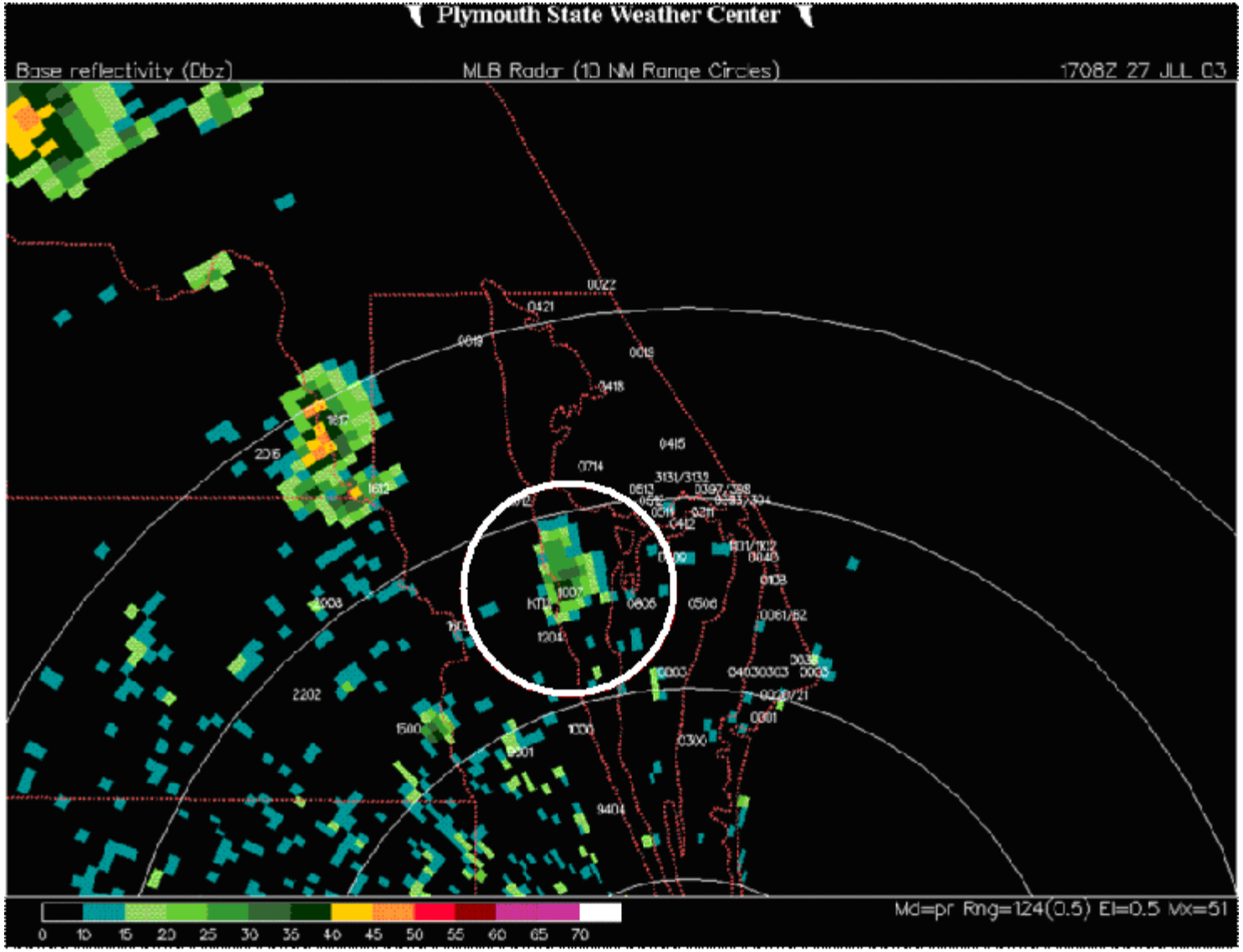

Figure 11. WSR-88D/MLB radar image around the time of the 21 knot maximum peak wind. The white numbers plotted indicate tower ID. The white circle indicates the location of the airmass thunderstorm which dissipated over Tower 1007 causing the high wind speed.

The WSR-88D/MLB radar showed a maximum reflectivity of around 50 dBZ in the line of cells at the time of outflow boundary generation. The cells that were triggered by the outflow boundary had reflectivity values of around 40 to 50 dBZ as seen in Figure 10. The line of cells was deemed to have a "weak/broken" strength due to their discontinuity and overall low reflectivity values.

There were 106 events studied that had peak winds from 35 to 49 knots. Thirty-seven percent of these events involved a sea breeze front/outflow boundary interaction, 31% had no such interaction, 19% had only an outflow boundary present, and 14% had only a sea breeze front present. The only other discernable trend was that the cell structure was linear over three quarters of the time.

5.2.3. Below-criteria Maximum Peak Wind Event (less than 35 knots)

The last case study to be covered was for a convective wind event which took place on 27 July 2003. At 1710 UTC, a maximum peak wind speed well below wind warning criteria was reported by Tower 1007 in the mesonetwork.

The event began with airmass thunderstorms forming in and around the mesonetwork. A lone cell slowly moved toward Tower 1007 and reached a maximum reflectivity of around 47 dBZ several minutes prior to producing the 21 knot maximum peak wind. The high wind report occurred just after the cell started to dissipate (Figure 11). This particular case study demonstrates the trend in convective events with below warning criteria maximum peak wind speeds. There is usually no outflow boundary or sea breeze front in the area and the cells generally are not organized in a line or a cluster.

6. Future Work

Future work will involve increasing the sample size of convective events to hopefully find specific differences in the setup (at the surface and aloft) for below-, at-, and well-above-criteria peak wind events. Knowing these differences will greatly help forecasters develop pattern recognition skills for predicting convective winds along Florida's Space coast. Additionally, Analysis of Variance (ANOVA) procedures will be completed for group direction, strength, and time-of-day.

We are also continuing to investigate a new thermodynamic-based index that we hope will improve convective wind predictions. This research is underway, but more time is needed to develop more complete results.

Related work is on-going to analyze the utility of some of the towers in the CCAFS/KSC mesonetwork (Koermer and Roeder, 2008). This is being done as part of the evaluation of the cost-effectiveness of these towers in supporting the 45 WS duties.

Other future projects might include a direct analysis of downburst speed decay with distance, fine-tuning the AMU WSR-88D cell trend tool for predicting downbursts (Wheeler 1998), developing dual polarization radar tools for downburst prediction for use with the new radar currently being acquired for use by 45 WS that is scheduled to become operational in late 2008.

7. Summary

Preliminary results from studying high resolution radar imagery overlaid with wind tower observations indicated that certain patterns can be used to determine the probability of high winds based on the statistics from a significant number of radar summaries during warning level criteria wind events. The results are summarized in Table 2. It was shown that for the majority of the events analyzed, cell initiation was due to sea breeze front and/or outflow boundary interactions. Linear forms of moderate strength cells traveling eastward accounted for a large percentage of the total number of events studied.

Table 2. Convective wind event criteria and forecasting characteristics.

Criteria	Forecasting Characteristics
< 35 knots	No organized SBF or OFB on radar No organized convection pattern Weaker single cell or cells Westward moving cell/cell group
35-49 knots	Weaker collision or interaction event Less solid linear/curved convection Radar visible SBF and/or OFB Weak/moderate cells Eastward, but sometimes westward moving cell/cell group
≥ 50 knots	Stronger collision or interaction event Solid linear/curved convection Radar visible SBF and/or OFB Moderate/strong cells Eastward moving cell/cell group

For the few occasions when there was either a high peak wind speed with a weak convective cell setup or a low peak wind speed with a strong convective cell setup, radiosonde data were analyzed to determine into what type of airmass

the downdraft fell. For the instances where the maximum peak wind was much stronger than expected, the sounding indicated an unsaturated layer from the surface to around 925 hPa with a saturated layer above.

The three case studies provided general examples of the conditions for well above-criteria, at-criteria, and below-criteria peak wind events. Strong events frequently needed a sea breeze front and outflow boundary interaction to form moderate to strong lines of cells. Also noted in this case study, was the fact that all but one of the 30 high convective wind events had an eastward component to the cell movement, which reiterates the climatology performed in previous studies of KSC/CCAFS convective wind events.

Much more detailed data, analyses, and many of these and additional references for these studies are available online at the following URL:

http://vortex.plymouth.edu/conv_winds/

8. Acknowledgements

This work was supported through the NASA Space Grant Program under the University of New Hampshire Subcontract 01-530. We would also like to thank NCDC, the Air Force 14th Weather Squadron, the Applied Meteorology Unit (AMU), and Computer Sciences Raytheon (CSR), who provided valuable archived data for our work. The Plymouth State University authors would also like to thank all personnel from the AMU and the 45WS, who supported their efforts while working at CCAFS during the summer of 2007.

9. References

Atkins, N. T., and R. M. Wakimoto, 1991: Wet microburst activity over the Southeastern United States: implications for forecasting. *Wea. Forecasting*, **6**, 470-482.

Boyd, B. F., W. P. Roeder, D. L. Hajek, and M. B. Wilson, 2005: Installation, upgrade, and evaluation of a short baseline Cloud-to-Ground Lightning Surveillance System used to support of space launch operations, *Conference on Meteorological Applications of Lightning Data*, 9-13 Jan 05, 4 pp.

Case, J. L., and W. H. Bauman III, 2004: A meso-climatology study of the high-resolution tower network over the Florida spaceport, *11th Conference on Aviation, Range, and Aerospace Meteorology,* 4-8 October 2004, P7.6.

Cummings, K. A., E. J. Dupont, A. N. Loconto, J. P. Koermer and W. P. Roeder, 2007. An updated warm-season convective wind climatology for the Florida space coast. Preprint CD-ROM, *16th Conf. of Applied Climatology*, 14-18 Jan 2007.

Harms, D. E., A. A. Guiffrida, B. F. Boyd, L. H. Gross, G. D. Strohm, R. M. Lucci, J. W. Weems, E. D. Priselac, K. Lammers, H. C. Herring and F. J. Merceret, 1999: The many lives of a meteorologist in support of space launch, *8th Conference On Aviation, Range, And Aerospace Meteorology,* 10-15 Jan 99, Dallas, TX, 5-9.

Koermer, J. P., and W. P. Roeder, 2008: Assessment of the importance of certain wind towers in the Cape Canaveral AFS/Kennedy Space Center mesonet for predicting convective winds, *13th Conference On Aviation, Range, And Aerospace Meteorology,* 21-24 Jan 08, New Orleans, LA.

Loconto, A. N., 2006: Improvements of warm-season convective wind forecasts at the Kennedy Space Center and Cape Canaveral Air Force Station. *M.S. Thesis*, Dept. of Chemical, Earth, Atmospheric and Physical Sciences, Plymouth State University, Plymouth, NH.

Loconto, A. N., J. P. Koermer, and W. P. Roeder, 2006: An updated warm-season convective wind climatology for Cape Canaveral Air Force Station/Kennedy Space Center, *12th Conference on Aviation Range and Aerospace Meteorology*, 30 Jan–2 Feb 2006, in Combined Preprint CDROM.

Mackey, J. B., 1998: Forecasting Wet Microbursts Associated With Summertime Airmass Thunderstorms Over The Southeastern United States, *M.S. Thesis*, Air Force Institute of Technology, AFIT/GM/ENP/98M-06, March 1998, 128 pp.

Proctor, F. H., 1989: Numerical simulation of an isolated microburst, Part-II: Sensitivity Experiments, J. Atmos. Sci., **46**, 2143-2165

Srivastava, R. C., 1985: A simple model of evaporatively driven downdraft: Application to microburst downdraft, J. Atmos. Sci., **42**, 1004-1023.

Wheeler, M. W., 1998: WSR-88D cell trends final report, *Applied Meteorology Memorandum*, Applied Meteorology Unit, ESCO Inc., Cocoa Beach. FL, http://science.ksc.nasa.gov/amu/, 1998, 36 pp.

Wheeler, M. W., and W. P. Roeder, 1996: Forecasting wet microbursts on the central Florida Atlantic Coast in support of the United States space program, *18th Conference on Severe Local Storms*, 19-23 February 1996, 654-658.